

Article

Data Fusion Based on Adaptive Interacting Multiple Model for GPS/INS Integrated Navigation System

Chuang Zhang, Chen Guo * and Daheng Zhang

Navigation College, Dalian Maritime University, Dalian 116026, China; zhchuangdmu@163.com (C.Z.); zhangdaheng@yeah.net (D.Z.)

* Correspondence: dmuguoc@126.com; Tel.: +86-189-0098-2551

Received: 11 August 2018; Accepted: 12 September 2018; Published: 17 September 2018



Abstract: The extended Kalman filter (EKF) as a primary integration scheme has been applied in the Global Positioning System (GPS) and inertial navigation system (INS) integrated system. Nevertheless, the inherent drawbacks of EKF contain not only instability caused by linearization, but also massive calculation of Jacobian matrix. To cope with this problem, the adaptive interacting multiple model (AIMM) filter method is proposed to enhance navigation performance. The soft-switching characteristic, which is provided by interacting multiple model algorithm, permits process noise to be converted between upper and lower limits, and the measurement covariance is regulated by Sage adaptive filtering on-line. Moreover, since the pseudo-range and Doppler observations need to be updated, an updating policy for classified measurement is considered. Finally, the performance of the GPS/INS integration method on the basis of AIMM is evaluated by a real ship, and comparison results demonstrate that AIMM could achieve a more position accuracy.

Keywords: ship; interacting multiple model; extended Kalman filter; GPS; inertial navigation system

1. Introduction

In general, the GPS/INS integrated system is combined with differential GPS in order to achieve higher accuracy [1]. This is basically because the inherent characteristics of high-precision differential GPS are better than the independent GPS mode. It is regrettable that this needs the presence of a correspondingly close base station, which not only restricts the scope of navigation but also spends more on construction of the base station. If GPS is combined with INS sensor, the former has the ability to give data about position and speed precisely, yet the latter has the capability to output data of attitude reliably. The integrated navigation system thus can conquer the drawbacks one another, while keeping the high-accuracy information.

If an inertial navigation system (INS) is integrated with GPS, GPS is mainly utilized for offsetting the accumulation errors of speed and position caused by INS, and the INS provides a better solution in the process of GPS signal unavailability [2,3]. Under the condition that the number of the available satellites rises to four and the influence of measurement noise is inconspicuous, credible solutions can be provided by GPS. This may be a significant flaw if GPS works independently. In general, three methods are used to restrain the problem, the first is exploiting INS with higher accuracy, the second is adding some accessory device, and the last is adopting advanced techniques and methods. In this thesis, the last two methods are united to ameliorate the better navigation solution.

The EKF [4], which is regarded as the most advanced method of integrating INS and GPS data, has been widely used for information fusion algorithms [5–8]. Under the condition that the noise is deemed as Gaussian, the nonlinear state and observation equations should be linearized according to the first-order Taylor series expansion. Nevertheless, higher order terms are ignored in the calculation process so EKF may not generate valid estimation of solutions, particularly when GPS interruption.

Especially for low-cost MEMS-based inertial measurement units (IMU), this case is even more common. The unscented Kalman filter (UKF) [9] was introduced as a linear regression estimation filter. In order to achieve the posterior mean and covariance precisely, UKF multiplies a deterministically group of sampling points which has suitable weights through the non-linear dynamic models and measurement models in the matter of any nonlinearity. It is very difficult to overcome weak points of assumption of Gaussian distribution to be tackled [10–12]. However, the capability of these improved KFs hinge upon the system being considered, and if the system has stronger nonlinear action, the accuracy of mode estimation will be poor. In the period of GPS signal unavailability, the navigation information based on KF diverges owing to process of linearization and inferior system model [13]. To address the shortcomings of KF-based methods mentioned above, many valuable efforts have been applied. A common approach for adjustment of covariance matrix on-line called innovation adaptive estimation can be used to solve the instability of KF-based methods, and then innovation adaptive estimation adaptive Kalman filtering (IAEAKF) [14–16] based on memory attenuation is present to prevent filtering divergence and reduce the influence of ambient noise. Also, residual sequences are applied to strengthen the random characteristics of filter on line. In order to enhance the estimation precision, adaptive filtering with fading memory algorithm is investigated. A new data fusion method is proposed to lessen risk of integrated vehicle health maintenance system (IVHMS). The purpose of complicated matrix operation in IVHMS is designed to dominate the time of high-order systems, which can be reduced by employing fuzzy Kalman filter (FKF). FKF is used to regulate performance. In terms of lessening IVHMS risk, this algorithm is a valid technique [17]. As an alternative, multiple model (MM) estimation was introduced. Amongst numerous MM estimate approaches, the interacting multiple model (IMM) filter, which is one of the highly effective state estimation algorithms, can be applied to multi-sensor data fusion [18–21]. Meanwhile, this approach is capable of estimating the state variables of a dynamic system with numerous behavior models as a probability switching approach. However, there are few real tests to verify its validity. In this paper, we present an enhanced adaptive IMM (AIMM) filter method for real sea trials.

This paper is organized as follows. Firstly, a full mathematical model of the SINS/GPS navigation system is analyzed. Then the AIMM method is proposed to increase performance of GPS/INS integrated navigation system, and the sea trial is applied to compare and analyze the performance of different kinds of integration methods. Lastly, main conclusions are offered and discussed.

2. SINS/GPS Fusion Model

2.1. System State Model

Based on the error model of INS, a more accurate dynamic model of systematic error is constructed to show that it is suitable for Kalman filter. For the sake of simplification, some relatively insignificant terms have been ignored in the process of linearization [22]. The psi-angle error models of INS can be expressed as [23]

$$\begin{cases} \delta \dot{p} = -\phi_{ne} \times \delta p + \delta s \\ \delta \dot{s} = -(2\phi_{ie} + \phi_{ne}) \times \delta s - \delta \vartheta \times \tau + \zeta \\ \delta \dot{\vartheta} = -(\phi_{ie} + \phi_{ne}) \times \delta \vartheta + \sigma \end{cases} \quad (1)$$

in which δp , δs , and $\delta \vartheta$ represent the position, speed, and orientation error vectors, respectively. ϕ_{ne} denotes the rate of navigation frame with respect to earth, and ϕ_{ie} denotes the rate of earth with respect to inertial frame. τ indicates the specific force vector. The systematic error of GPS/INS integrated system is achieved through expansions from both the accelerometer bias error vector ζ and the gyro drift error vector σ .

Compared with the INS/GPS integrated system, resemble precision of system state estimation is proposed on the basis of increasingly wide utilization of error states for the EKF. Nevertheless, if a total states model of UKF is utilized, every output data of system strapdown processing which contains each sampling point will be obliged to be repeated, and then the additional computational cost will be

increased greatly. Hence, the error states of INS/GPS integrated system can be utilized and expressed as follows [24].

$$\begin{cases} X_{Nav} = [\delta P_N, \delta P_E, \delta P_D, \delta V_N, \delta V_E, \delta V_D, \delta \theta_N, \delta \theta_E, \delta \theta_D]^T \\ X_{Acc} = [\zeta_{bx}, \zeta_{by}, \zeta_{bz}, \zeta_{fx}, \zeta_{fy}, \zeta_{fz}]^T \\ X_{Gyro} = [\sigma_{bx}, \sigma_{by}, \sigma_{bz}, \sigma_{fx}, \sigma_{fy}, \sigma_{fz}]^T \\ X_{Ant} = [\delta l_{bx}, \delta l_{by}, \delta l_{bz}]^T \end{cases} \quad (2)$$

in which $\delta P_N, \delta P_E, \delta P_D$ denote the three-dimension position error; $\delta V_N, \delta V_E, \delta V_D$ denote the velocity error; and $\delta \theta_N, \delta \theta_E, \delta \theta_D$, denote orientation error, respectively. The nine navigation error vectors are represented by the north-east-down (NED) navigation frame. $\zeta_{bx}, \zeta_{by}, \zeta_{bz}, \zeta_{fx}, \zeta_{fy}, \zeta_{fz}$ denote accelerometer error vectors; and $\sigma_{bx}, \sigma_{by}, \sigma_{bz}, \sigma_{fx}, \sigma_{fy}, \sigma_{fz}$ denote gyro sensor errors vector. $\delta l_{bx}, \delta l_{by}, \delta l_{bz}$ denote lever arm errors.

2.2. Measurement Model

Within the tightly coupled integration model, the measurement state vector of KF is constructed by the relation between the INS derived measurements and GPS raw observables. The GPS observables can be basically implemented with three different measurements, such as carrier phase, pseudo-range and Doppler. In order to obtain high accuracy results, the carrier phase measurements have to be used in the filter update. Considering this fact, in this paper the dual-differential (DD) pseudo-range data and single-differential (SD) Doppler data, which can be implemented in the integration system, will be used. The GPS measurement model can be described as

$$\begin{cases} \Delta \nabla \rho_{GPS}^e - \Delta \nabla \rho_{INS}^e = H^e C_n^e \delta r + H^e C_b^e \delta L^b + \Delta \nabla \varepsilon_\rho \\ \nabla D_{GPS}^e - \Delta D_{INS}^e = \frac{1}{\lambda_{GPS}} H^e C_n^e \delta v + \nabla \varepsilon_D \end{cases} \quad (3)$$

in which ∇ stands for differential value between two adjacent satellites and $\Delta \nabla$ represents the double differential arithmetic; D_{GPS}^e and ρ_{GPS}^e refer to GPS Doppler and pseudo-range observables, respectively; D_{INS}^e and ρ_{INS}^e indicate the Doppler and pseudo-range data given by INS, respectively; ε_ρ and ε_D indicate the pseudo-range and Doppler data of measurement noise, respectively; H^e denotes the geometry transform matrix; C_n^e denotes the rotation matrix from navigation frame to earth frame; C_b^e denotes the rotation matrix from body frame to earth frame; and λ_{GPS} denotes the wavelength of GPS signal.

Because of the uncertainty of lever arm, deviation between IMU physical center and GPS antenna should be considered, especially under the conditions that the value of IMU prediction needs to be updated. The IMU position originates from GPS position in the e-frame.

$$r_{GPS}^e = r_{INS}^e + C_b^e L^b \quad (4)$$

in which L^b means the lever arm deviation vector within the body coordinate frame.

Analogously, the relationship between the IMU speed and the GPS antenna

$$v_{GPS}^e = C_n^e v_{INS}^e + C_b^e (\Omega_{ib}^b - \Omega_{in}^b) L^b \quad (5)$$

2.3. SINS/GPS Fusion with EKF

An extension of the KF (EKF) can be used in this paper in order to unite the output of inertial unit and GPS measurements. An analytical solution of EKF is a recursive process that contains a prediction step that can be written as [25]

$$\begin{cases} x_m^- = \Phi_{m,m-1} x_{m-1}^+ \\ P_m^- = \Phi_{m,m-1} P_{m-1}^+ \Phi_{m,m-1}^T + Q_{m-1} \end{cases} \quad (6)$$

in which x_{m-1}^+ and x_m^- denote the posteriori state vector at time $m - 1$ and the priori state vector at time m , respectively; $\Phi_{m,m-1}$ stands for the discrete state transfer matrix from time $m - 1$ to m ; P_{m-1}^+ and P_m^- represent the posteriori covariance matrix of x_{m-1}^+ and the priori covariance matrix of x_m^- ; and then Q_{m-1} denotes the process noise covariance matrix. The correction procedure is determined by

$$\begin{cases} G_m = P_m^- D_m^T (H_m P_m^- D_m^T + C_m)^{-1} \\ x_m^+ = x_m^- + G_m (R_m - D_m x_m^-) \\ P_m^+ = (I - G_m D_m) P_m^- \end{cases} \quad (7)$$

in which G_m denotes the Kalman gain; x_m^+ represents posteriori state vector at time m ; R_m and D_m indicate the measurement residual vector and measurement design matrix, respectively; and C_m represents the covariance matrix of measurement noise.

The estimated navigation parameters may be updated, provided that the GPS measurements are available, and thus, the predicted errors of sensor will be applied to modify the original inertial measurements.

Generally speaking, Kalman filter can provide a better solution according to the correct statistics of process noise and measurement noise. However, under the conditions that the mathematical models are subject to uncertainty or the off-centered Gaussian noise do not influence the process model and measurement model, both Kalman filtering and KF-based derivation methods cannot provide convincing results.

3. System Architecture

The proposed adaptive IMM filter method in this study is applied to evaluate the GPS/INS combined data. These independent dynamic equations, including process noises of various sorts, are performed synchronously. Meanwhile, the covariance of measurement noise on the basis of residual information method is recursively applied. Aiming to curb the uncertainty process noise and measurement noise synchronously, the AIMM filter is introduced.

3.1. Interacting Multiple Model Filter Structure

The IMM filter, which compared with other multiple model estimation algorithms, has attracted wide attention in virtue of their higher performance and lower computational cost [26,27]. Therefore, the IMM estimator has used to obtain the state estimates under various filters on the basis of the model probabilities in this research. The IMM filter method is composed of three parts: interaction and mixing, mode probability update, and combination.

3.1.1. Interaction and Mixing

Initially, the system can be considered as a discrete group of r models, which can be represented as $M = \{M_1, M_2, \dots, M_r\}$. The mixing probability μ_m^{ij} can be described as

$$\mu_m^{ij} = \frac{1}{\bar{c}_j} p_{ij} \mu_{m-1}^i \quad (8)$$

in which μ_{m-1}^i is the mode probability of model i in the preceding stage and p_{ij} is the mode switching probability matrix.

A normalizing factor \bar{c}_j can be denoted by

$$\bar{c}_j = \sum_{i=1}^r p_{ij} \mu_{m-1}^i \quad (9)$$

The initial mixed state estimate $x_{m-1}^{0,j}$ and its covariance $P_{m-1}^{0,j}$ for each filter can be expressed as

$$x_{m-1}^{0,j} = \sum_{i=1}^r \mu_m^{i|j} x_{m-1}^{+,i} \tag{10}$$

$$P_{m-1}^{0,j} = \sum_{i=1}^r \mu_m^{i|j} \left[P_{m-1}^{+,i} + (x_{m-1}^{+,i} - x_{m-1}^{+,j})(x_{m-1}^{+,i} - x_{m-1}^{+,j})^T \right] \tag{11}$$

in which $x_{m-1}^{+,i}$ and $P_{m-1}^{+,i}$ are the final mean and covariance for a single model i , respectively.

3.1.2. Mode Probability Update

Applying the original mixed state estimate and covariance of preliminary procedure, the likelihood of KF prediction and update for each filter is obtained, and the state mean and covariance of each filter can be estimated accordingly. Furthermore, the function of likelihood which stems from every filter can be simplified as

$$\Lambda_m^i = \frac{1}{(2\pi)^{n/2} |S_m^i|^{1/2}} \exp\left(-\left(v_m^i\right)^T \left(S_m^i\right)^{-1} v_m^i / 2\right) \tag{12}$$

in which n represents the frequency of measurements in this step; v_m^i and S_m^i are the innovation sequence and its corresponding covariance, respectively, which are calculated as

$$v_m = z_m - H_m x_m^- \tag{13}$$

$$S_m = H_m P_m^- H_m^T + R_m \tag{14}$$

The updated probability of each filter can be written as

$$\mu_m^i = \frac{1}{c} \Lambda_m^i \bar{c}_i \tag{15}$$

in which c indicates a normalized constant for the mode probability update, and is done as

$$c = \sum_{i=1}^r \Lambda_m^i \bar{c}_i \tag{16}$$

3.1.3. Combination

Now, the prediction for the next step would be gotten according to the updated probability of each filter. Under the hybrid formula, the final integrated state estimates x_m and its covariance P_m can be computed as

$$x_m = \sum_{i=1}^r \mu_m^i x_m^i \tag{17}$$

$$P_m = \sum_{i=1}^r \mu_m^i \left[P_m^{+,i} + (x_m^{+,i} - x_m)(x_m^{+,i} - x_m)^T \right] \tag{18}$$

3.2. Adaptive Kalman Filtering

The numerical value of measured noise varies with time due to the influence of the surrounding environment in the practical applications of GPS/INS integrated navigation system. In order to enhance the performance of positioning, it is necessary to adjust the statistical data of the measured

variance matrix on line. In addition, under the condition of process noise is known, the Sage filtering method is applied to adjust the measured variance.

$$R_m = (1 - d_m)R_{m-1} + d_m(e_m e_m^T + H_m P_m H_m^T) \tag{19}$$

$$d_m = \frac{(1 - b)}{(1 - b^m)} \tag{20}$$

in which $b \in [0.95, 0.99]$ is a forgetting factor, and in this paper it is set to 0.97 according to data analysis. The residual sequence e_k is expressed using the following relationship

$$e_m = z_m - H_m x_m \tag{21}$$

It should be noted that the abnormal errors of the observations are removed firstly during practical applications.

3.3. GPS/INS Integrated Architecture

In this paper, code and Doppler observations from GPS is combined with INS predicted observations in tightly coupled architecture. Figure 1 shows the block diagram of INS/GPS tightly-coupled integration with AIMM algorithm. The IMU outputs the angular rate and specific force provided by gyroscopes and accelerometers, respectively, which are corrected by the estimated states of sensor error, and now it is used to integrated navigation system and implements INS mechanization.

In view of statistic uncertainties of process noise, up and down edges of process noise covariance are conducted in the IMM filter. Within any time stage, the mixture probabilistic in the IMM filter are given in the process of interaction step, then the state estimates of every filter are computed in the process of time updating stage of EKF.

To mitigate the atmospheric errors, double differenced is used for the GPS code and Doppler observations. In the update of the measure data process, the updating methods can be executed by taking into consideration the measure values with the identical kind in every filtering stage with U-D filter; in other words, both code rate and Doppler measure values of GPS in diverse frequency channels are updated orderly.

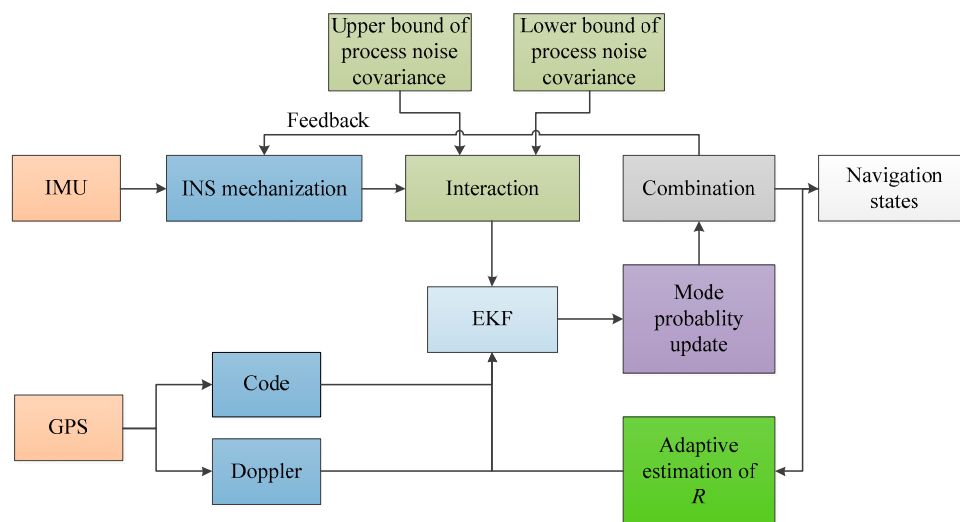


Figure 1. Flowchart of INS/GPS tightly-coupled integration with AIMM algorithm.

Every filter would implement the prediction and updating stages on condition that GPS observed value and INS provided observed value are given. When the measurement update is accomplished, the mode probability will be updated. A weighting group that the status is updated from the

dual-model IMM filter is calculated, then the ultimate integrated navigation solution is fulfilled in the light of the hybrid formulations. Meanwhile, the measurement noise covariance can be updated by making use of the residual data. Ultimately, the error states vector of sensor, which are estimated in IMM filter, are fed into INS mechanization stage for the sake of offsetting inertial original outputs.

4. Real Ship Experiment and Its Performance Analysis

4.1. Real Ship Experiment Description

A real ship experiment was executed near Dalian bay and adjacent area, China. The performance of the developed navigation solution is tested and verified by using ship-mounted experimental data. An ordinary navigation grade IMU, whose sensor specifications can be found in Table 1, and one high-grade GPS receivers were used to collect data. Figure 2 indicates sea trail trajectory in Dalian bay. The whole sailing time of sea trial was about 21 h, the ship is in continuous sailing and the distance travelled is about 200 n mile. Only a sea trial of about 50 min (red circle) is selected.

Table 1. IMU specifications

Gyroscope		Accelerometer	
Bias offset	$\pm 20^\circ/\text{h}$	Bias offset	$\pm 50 \text{ mg}$
Bias repeatability	$< \pm 1^\circ/\text{h}$	Bias repeatability	$\pm 0.75 \text{ mg}$
In run stability	$1^\circ/\text{h} (1\sigma)$	In run stability	$0.25 \text{ mg} (1\sigma)$
Scale factor	1500 ppm	Scale factor	4000 ppm
Angle random walk	$0.0667^\circ/\sqrt{h}$	Velocity random walk	$55 \text{ mg}^\circ/\sqrt{Hz}$

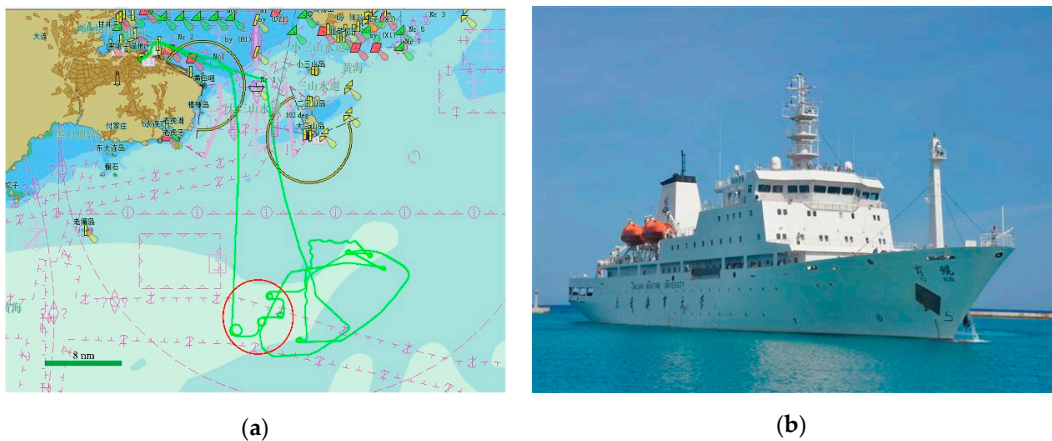


Figure 2. Sea trail trajectory in Dalian port. (a) Sea trail trajectory. (b) Experimental ship.

For the sake of implement the performance assessment of the GPS/INS integrated system, the single frequency pseudo-range and Doppler measured value provided by GPS are applied. The reference solution is attained through IMU measured value combine with differential GPS (DGPS) carrier phase measured value, result in a high location accuracy level will be achieved for the algorithm evaluation.

4.2. Simulation Results and Analysis

For the sake of verify the performance of AIMM filter, this paper execute the simulation test which is given by

$$\begin{cases} x_m = k_1 x_{m-1} - k_2 + \lambda_m^1 & \text{if } m \leq t/2 \\ x_m = k_3 x_{m-1}^{k_4} + x_{m-1} + \lambda_m^2 & \text{otherwise} \\ y_m = -4x_m^{(1/2)} + \rho_m \end{cases} \quad (22)$$

in which t denotes the time interval, x_m and y_m denote state and measurement series, respectively. $i = 1, 2$, $\lambda_m^i \sim N(0, \sigma_\lambda^2)$, $\sigma_\lambda = 0.002$, and $\rho_m \sim N(0, \sigma_\rho^2)$ indicate sequences with Gaussian white noises nonzero mean. $k_1 = 0.986$, $k_2 = 0.31$, $k_3 = 0.001$, $k_4 = 0.835$. $x_0 \sim N(20, \sigma_\lambda)$.

$$[p_{ij}] = \begin{bmatrix} 0.9943 & 0.0057 \\ 0 & 1.0000 \end{bmatrix} \tag{23}$$

As shown in Figure 3, the state estimation information is displayed utilizing the IMM filter and AIMM filter. The improvement obtained on the basis of combining the adaptive systems can be seen in Figure 4 that describes the model probability of two types of filter modes. The upper image of Figure 4 indicates the result of IMM filter while another image denotes output of AIMM filter. As it can be seen in Figure 4, that the prevailing Model 1 of m_p take place by turn with Model 2 prior to the time of expectation ($t = 150$). So Model 2 can be affected by estimated value of IMM filter. The situation is very similar after $t = 150$, and Model 1 remains predominant. Another image of Figure 4 indicates that there is a transition delay of Model 1 with regard to Model 2. It is mainly because of the existence of noise measuring data that makes it difficult to achieve the estimated state vector of every filter. Moreover, as shown in Figure 3, the state estimation generated by AIMM filter is superior to the IMM filter.

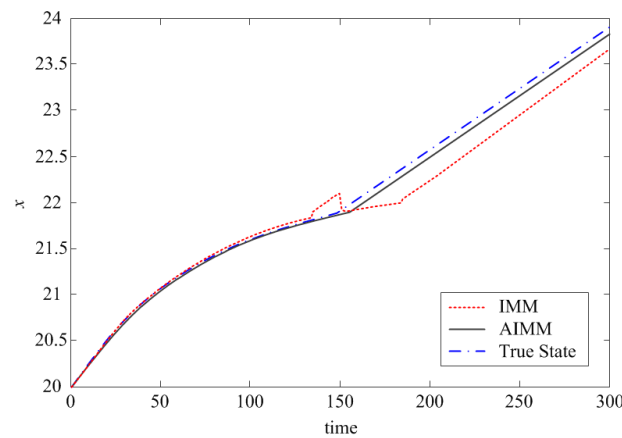
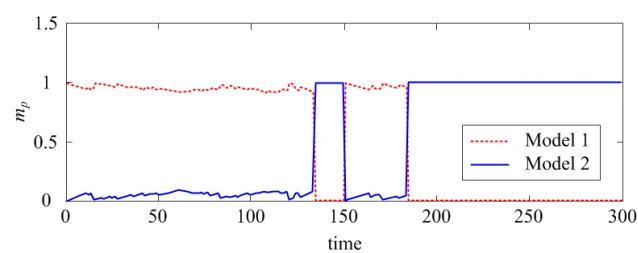
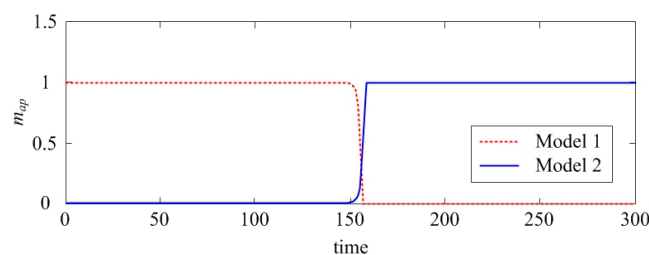


Figure 3. State estimation of IMM and AIMM.



(a)



(b)

Figure 4. Model probability of IMM and AIMM. (a) Model probability of IMM. (b) Model probability of AIMM.

4.3. Performance Analysis and Comparison of Proposed Algorithm

To verify the performance of the proposed algorithm, the effectiveness of the proposed algorithm is testified by GPS is fused with low-cost INS. We investigate an alternative to the EKF, IMM filter, and AIMM filter data fusion technology with regard to the marine integrated navigation system, and INS/GPS integrated navigation system makes the most of the complete mathematical equations which contain the pseudo-range and Doppler measure value and INS provided measure value.

The priori elevation dependent weighting method is described by the undifferenced measurement covariance at concrete elevation (el)

$$r_{ii} = \sigma_0^2 / (\sin(\text{el}))^2 \quad (24)$$

in which σ_0 represents the standard deviation, 0.3 m with regard to pseudo-ranges and 0.01 m/s with regard to Doppler observing data. First, an adaptive algorithm, which estimates the measurement covariance on line, is employed to enhance performance. Then, KF based on U-D filter will be introduced to update the filter with pseudo-range and Doppler observing data.

In general, establishing a precise randomness model with regard to INS, which works better under various conditions, is very difficult. For addressing this problem, we not only propose a dual-model IMM filter method, but also set two process noise covariance matrices, namely, $Q_1 = 4Q_0$ and $Q_s = 0.25Q_0$. Where Q_0 is nominal covariance, which could be determined on the basis of the sensor detailed parameters.

The dual-model IMM filter method was used when the preset value are confirmed by empirical data according to theory of probability. These probabilities can be represented as a Markov chain transfer matrix between these models

$$[p_{ii}] = \begin{bmatrix} 0.98 & 0.02 \\ 0.02 & 0.98 \end{bmatrix} \quad (25)$$

In fact, these values have little effect on the final results. With the aim to ameliorate the stability of the filter in the initial phase, it is crucial to consider the initial model probability of large process noise mode is a little larger. The initial model probabilities are 0.4 with regard to small process noise model, while 0.6 for large process noise model.

Figure 5 shows a time series of positioning errors in the north, east, and down directions based on GPS/INS integration configurations. For purpose of testing the performance of AIMM filter, EKF and IMM with GPS/INS configuration are employed. As far as the positioning accuracy is concerned, the proposed adaptive IMM filter method reach significantly better results than the EKF and IMM filter method. Due to the imprecise statistical characteristics of the dynamic model and the measurement model, the EKF solutions comprise too much noise. Although a smoother track is shown from the navigation solution of AIMM filter, some abrupt positioning errors can be eliminated in the EKF framework. Furthermore, the traditional IMM filter fulfills lower precision if the priori measurement noise covariance is imprecise.

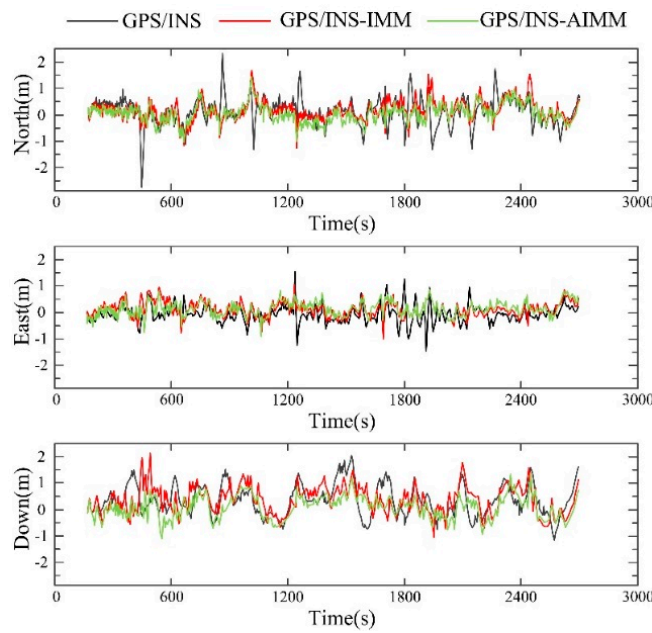


Figure 5. Comparison of position accuracy among different filters.

In about 200–600 s, the navigation solution rapidly deviated from a 0.5 m error to almost a 3 m error. This is principally because multipath has the great ability of interference, and then the abnormal effects had done a great deal to influence the overweighed pseudo-range. Therefore, the positioning precision provided by GPS/INS-AIMM has a certain improvement for GPS/INS-IMM and GPS/INS.

Figure 6 describes the position RMS (root mean square) error for EKF, IMM, and AIMM filters. As is evident from Figure 6, the AIMM can be ameliorate the positioning solutions of GPS/INS integrated navigation by 35.4%, 37.1%, and 31.7% in the north, east and down directions, respectively, in comparison with EKF filter. It is evident from the figure that east direction accomplishes the optimal performance owing to geometric configuration. Also, the AIMM solutions achieve the percentage improvement of 22.2%, 31.8%, and 11.9%, respectively, when IMM filter is used. The IMM filter provides good performance in comparison with EKF, but inadequate knowledge of measurement noise restricts the accuracy.

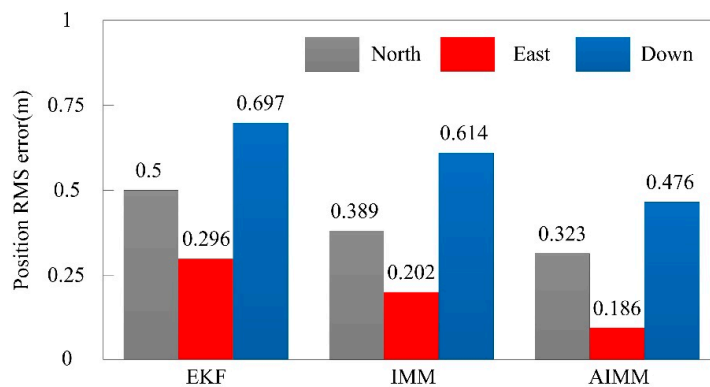


Figure 6. Position RMS error for EKF, IMM, and AIMM filters.

Figure 7 illustrates the velocity and velocity errors from the combination of GPS and INS sensor measurements by using AIMM. It can be concluded that AIMM model obtain centimeter/second level accuracy in north, east, and down components. Nevertheless, it has a maximum error of 0.27 m/s which is owing to the vessel steering.

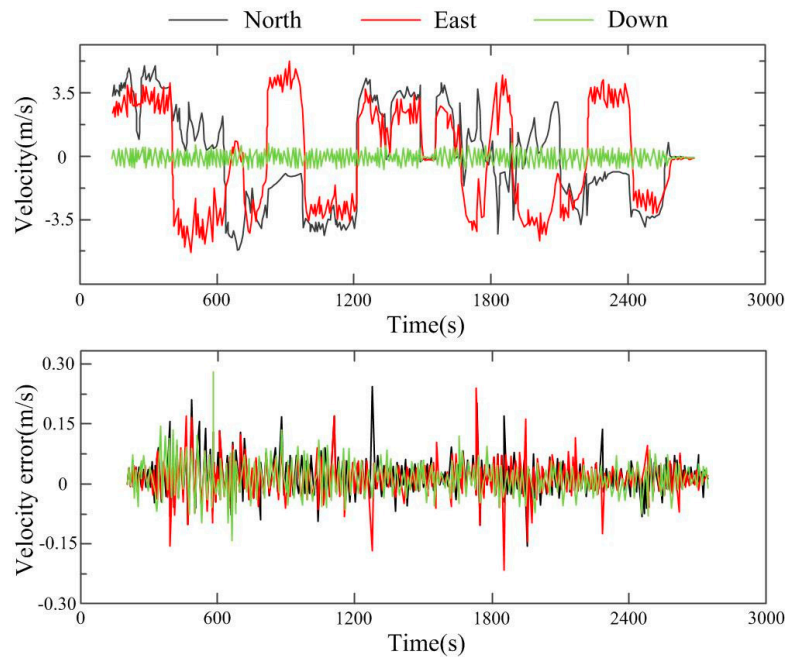


Figure 7. Velocity and velocity errors based on AIMM filter.

Figure 8 plots the velocity RMS errors for different filters. It can be shown the AIMM filter is able to perform well in east and north directions in comparison with EKF filter. Compared to the EKF filter, the proposed AIMM filter ameliorates the velocity solutions in the north and east components by 55% and 47.4%, respectively; despite a slight drop in the down component.

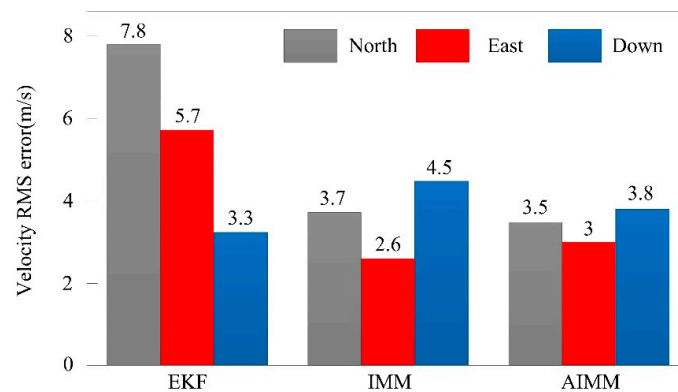


Figure 8. Velocity RMS errors for different filters.

Figure 9 describes a performances comparison about attitude and attitude errors by using AIMM filter. From the comparison results we can see that the precision of roll and pitch are obviously higher than the heading precision. Figure 10 also proves that AIMM has better performance in attitude estimation than EKF. Attitude accuracy of IMM has similar performance compared with AIMM.

Figure 11 describes the model probability of the AIMM filter. The AIMM use the model probability to check the filter switching capability. The ability of soft-switching allows the filter to switch autonomously between upper and lower limits of Q_k ; and it tracks the vessel motional trend.

Table 2 summarizes the comparisons of three different methods. For the position RMS error, the IMM filter provides better performances in comparison with EKF and IMM. It can be shown that the AIMM filter is able to perform well in east and north directions in comparison with EKF filter and IMM for the velocity RMS error. In terms of attitude RMS error, both AIMM and IMM have better performance in attitude estimation than EKF.

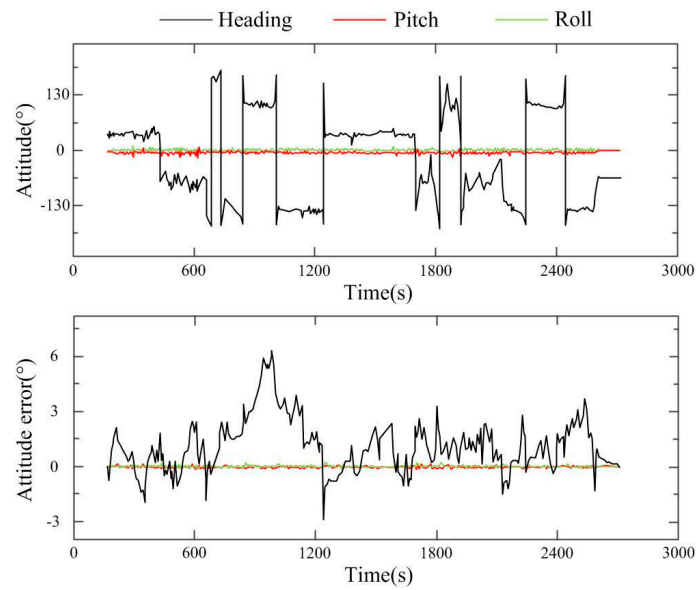


Figure 9. Attitude and attitude errors based on AIMM filter.

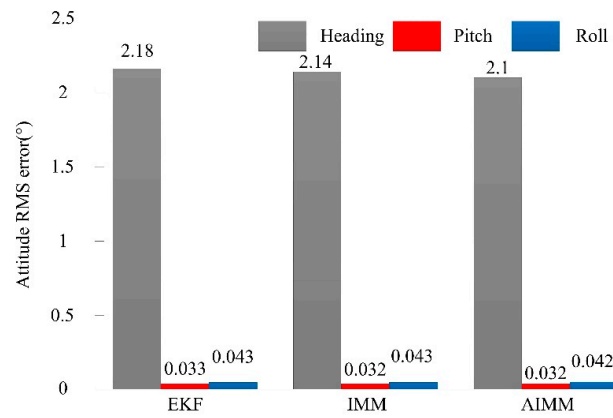


Figure 10. Attitude RMS errors for different filters.

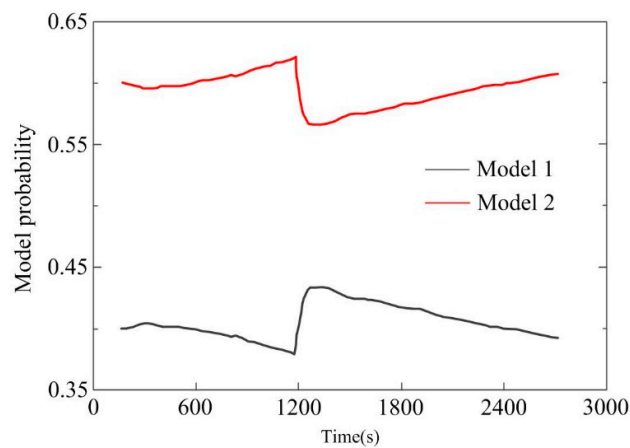


Figure 11. Model probability in the AIMM filter.

Table 2. Comparisons of three different methods.

	Position RMS Error			Velocity RMS Error			Attitude RMS Error		
	North	East	Down	North	East	Down	Heading	Pitch	Roll
EKF	0.5	0.296	0.697	7.8	5.7	3.3	2.18	0.033	0.043
IMM	0.389	0.202	0.614	3.7	2.6	4.5	2.14	0.032	0.043
AIMM	0.323	0.186	0.476	3.5	3	3.8	2.1	0.032	0.042

5. Conclusions

The major contribution of this work is to propose an AIMM filter approach which is the integration of INS/GPS in sensor data fusion for sea trial in Dalian port, China. It is employed to solve the problem of precision decrease affected by noise nondeterminacy of EKF. The estimation accuracy was enhanced as the AIMM filter ought to separately adjust the covariance between process noise and measurement noise. In addition, in order to decrease computational load, a measurement particular sequential update method was adopted. The results gained from real ship experiments and simulations demonstrate that GPS/INS integration method can be achieve a better position precision.

In the future, this topic will be concentrated in the integration of multi-GNSS and INS for enhancing positioning precision and eliminating equivocal resolution ability. Moreover, the advanced algorithm of data fusion will be considered.

Author Contributions: C.Z. and C.G. conceived and designed the experiments; D.Z. performed the experiments; C.Z. analyzed the data; D.Z. contributed analysis tools; C.Z. wrote the paper.

Funding: This research was funded by [the National Nature Science Foundation of China] grant number [51579024, 51879027], [the National Science Fund of Liaoning Province] grant number [20170520243], [the Fundamental Research Funds for the Central Universities] grant number [3132018154].

Conflicts of Interest: The authors declare no conflict of interest.

References

- Georgy, J.; Karamat, T.; Iqbal, U.; Noureldin, A. Enhanced MEMS-IMU/odometer/GPS Integration using Mixture Particle Filter. *GPS Solut.* **2011**, *15*, 239–252. [[CrossRef](#)]
- Liu, Y.; Fan, X.; Lv, C.; Wu, J.; Li, L. An Innovative Information Fusion Method with Adaptive Kalman Filter for Integrated INS/GPS Navigation of Autonomous Vehicles. *Mech. Syst. Signal Process.* **2017**, *100*, 605–616. [[CrossRef](#)]
- Han, S.; Wang, J. Integrated GPS/INS navigation system with dual-rate Kalman filter. *GPS Solut.* **2012**, *16*, 389–404. [[CrossRef](#)]
- Cheng, J.; Yang, L.; Li, Y.; Zhang, W. Seamless outdoor/indoor navigation with wifi/gps aided low cost inertial navigation system. *Phys. Commun.* **2014**, *13*, 31–43. [[CrossRef](#)]
- Huang, J.; Tan, H.S. A low-order DGPS-based vehicle positioning system under urban environment. *IEEE/ASME Trans. Mechatron.* **2006**, *11*, 567–575. [[CrossRef](#)]
- Rezaei, S.; Sengupta, R. Kalman filter-based integration of DGPS and vehicle sensors for localization. *IEEE Trans. Control Syst. Technol.* **2007**, *15*, 1080–1088. [[CrossRef](#)]
- Fiengo, G.; Di Domenico, D.; Glielmo, L. A hybrid procedure strategy for vehicle localization system: Design and prototyping. *Control Eng. Pract.* **2009**, *17*, 14–25. [[CrossRef](#)]
- Cui, Y.; Ge, S.S. Autonomous vehicle positioning with GPS in urban canyon environments. *IEEE Trans. Robot. Autom.* **2003**, *19*, 15–25. [[CrossRef](#)]
- Han, H.; Wang, J.; Wang, J.; Moraleda, A.H. Reliable partial ambiguity resolution for single-frequency gps/bds and ins integration. *GPS Solut.* **2016**, *21*, 1–14. [[CrossRef](#)]
- Daum, F. Nonlinear Filters: Beyond the Kalman Filter. *IEEE Trans. Aerosp. Electron. Syst.* **2005**, *20*, 57–69. [[CrossRef](#)]
- Chen, S.Y. Kalman Filter for Robot Vision: A Survey. *IEEE Trans. Ind. Electron.* **2012**, *59*, 4409–4420. [[CrossRef](#)]
- Loiola, M.B.; Lopes, R.R.; Romano, J.M.T. Modified Kalman Filters for Channel Estimation in Orthogonal Space-time Coded Systems. *IEEE Trans. Signal Process.* **2011**, *60*, 533–538. [[CrossRef](#)]

13. Roshany-Yamchi, S.; Cychowski, M.; Negenborn, R.R.; Schutter, B.D.; Delaney, K.; Connell, J. Kalman Filter-based Distributed Predictive Control of Large-scale Multi-rate Systems: Application to Power Networks. *IEEE Trans. Control Syst. Technol.* **2012**, *21*, 27–39. [[CrossRef](#)]
14. Zhang, C.; Guo, C.; Zhang, D.H. Ship Navigation via GPS/IMU/LOG Integration using Adaptive Fission Particle Filter. *Ocean Eng.* **2018**, *156*, 435–445. [[CrossRef](#)]
15. Hide, C.; Moore, T.; Smith, M. Adaptive Kalman filtering for low-cost INS/GPS. *J. Navig.* **2003**, *56*, 143–152. [[CrossRef](#)]
16. Hu, C.; Chen, W.; Chen, Y.; Liu, D. Adaptive kalman filtering for vehicle navigation. *J. Glob. Position. Syst.* **2003**, *2*, 42–47. [[CrossRef](#)]
17. Rodger, J.A. Toward reducing failure risk in an integrated vehicle health maintenance system: A fuzzy multi-sensor data fusion Kalman filter approach for IVHMS. *Expert Syst. Appl.* **2012**, *39*, 9821–9836. [[CrossRef](#)]
18. Toledo-Moreo, R.; Zamora-Izquierdo, M.A.; Ubeda-Minarro, B.; Gomez-Skarmeta, A.F. High-integrity IMM-EKF-based road vehicle navigation with low-cost GPS/SBAS/INS. *IEEE Trans. Intell. Transp. Syst.* **2007**, *8*, 491–511. [[CrossRef](#)]
19. Tsunashima, H.; Murakami, M.; Miyata, J. Vehicle and road state estimation using interacting multiple model approach. *Veh. Syst. Dyn.* **2006**, *44*, 750–758. [[CrossRef](#)]
20. Cosme, L.B.; Caminhas, W.M.; D'Angelo, M.F.; Palhares, R.M. A novel fault prognostic approach based on interacting multiple model filters and fuzzy systems. *IEEE Trans. Ind. Electron.* **2018**, *99*, 1–10. [[CrossRef](#)]
21. Wang, L.; Li, S. Enhanced multi-sensor data fusion methodology based on multiple model estimation for integrated navigation system. *Int. J. Control Autom.* **2018**, *3*, 1–11. [[CrossRef](#)]
22. Titterton, D.; Weston, J. Strapdown inertial navigation technology. *IEEE Trans. Aerosp. Electron. Syst.* **2004**, *20*, 33–34. [[CrossRef](#)]
23. Han, H.; Wang, J.; Mingyi, D.U. GPS/BDS/INS tightly coupled integration accuracy improvement using an improved adaptive interacting multiple model with classified measurement update. *Chin. J. Aeronaut.* **2018**, *3*, 556–566. [[CrossRef](#)]
24. Ji, H.R.; Gankhuyag, G.; Chong, K.T. Navigation system heading and position accuracy improvement through gps and ins data fusion. *J. Sens.* **2016**, *3*, 1–6. [[CrossRef](#)]
25. Jo, K.; Chu, K.; Sunwoo, M. Interacting multiple model filter-based sensor fusion of gps with in-vehicle sensors for real-time vehicle positioning. *IEEE Trans. Intell. Transp. Syst.* **2012**, *13*, 329–343. [[CrossRef](#)]
26. Compare, M.; Baraldi, P.; Turati, P.; Zio, E. Interacting multiple-models, state augmented particle filtering for fault diagnostics. *Probab. Eng. Mech.* **2015**, *40*, 12–24. [[CrossRef](#)]
27. Chalvatzaki, G.; Papageorgiou, X.S.; Tzafestas, C.S.; Maragos, P. Augmented human state estimation using interacting multiple model particle filters with probabilistic data association. *IEEE Trans. Robot. Autom.* **2018**, *99*, 1–8. [[CrossRef](#)]

